Double-Pulse Characterization of GaN Monolithic Bidirectional Switches in Single Stage OBC

Guanjiang Liu[1], Qishan Pan[1], Xinxu Cui[1], Haoyu Wang[1,2]
1 School of Information Science and Technology, ShanghaiTech University, Shanghai, China
2 Shanghai Engineering Research Center of Energy Efficient and Custom AI IC, Shanghai, China
wanghy@shanghaitech.edu.cn

***Abstract*—GaN monolithic bidirectional switches (MBDSs) are ideal for single-stage on-board chargers due to their compact size and fast switching. However, conducting a conventional double-pulse test (DPT) on MBDSs causes destructive overvoltage because off-state MBDSs lack passive third-quadrant conduction, To resolve this for high-current testing, we propose a customized DPT with a tailored gating sequence to ensure a continuous freewheeling path. Using a low-parasitic-inductance tewstbed, we safely evaluated the devices up to 50 A. Results show highly symmetrical switching under both positive and negative voltage stress. Furthermore, owing to its fast switching, minimal PCB footprint and parasitic inductance, the GaN MBDS exhibits lower switching losses than SiC devices and significantly reduced voltage overshoot compared with its non-monolithic GaN equivalents.**

***Index Terms*—Double-pulse testing, electric vehicle charging, GaN monolithic bidirectional switches, single-stage on-board chargers**

I. Introduction

Electric vehicle on-board chargers (OBCs) increasingly demand higher power density, efficiency, and reliability. Conventional two-stage OBCs cascade an active power-factor-correction stage with an isolated DC/DC stage, requiring a bulky intermediate DC-link electrolytic capacitor to buffer twice the line-frequency power [1]. Conversely, single-stage architectures reduce or eliminate the need for this capacitor by integrating AC/DC conversion, isolation, and regulation, thereby improving volumetric power density [2]. Consequently, single-stage OBCs are attracting significant interest from both industry and academia.

Single-stage isolated OBCs, particularly dual-active-bridge (DAB) and AC-link topologies, require four-quadrant switches to control bidirectional current and voltage blocking for high-frequency power transfer and grid-current shaping [3], [4]. These switches are traditionally realized using a diode bridge with a single switch or anti-series configuration (common drain or common source), alongside emerging wide–band-gap implementations [5].

Recently, GaN monolithic bidirectional switches (MBDSs) have become highly attractive for high-density OBCs due to their low parasitic charge, fast switching, and compact footprint [6]. However, these high-performance attributes also make MBDS dynamic behavior highly sensitive to device structure, commutation quadrants, parasitics, and gate-drive strategies, necessitating rigorous characterization.

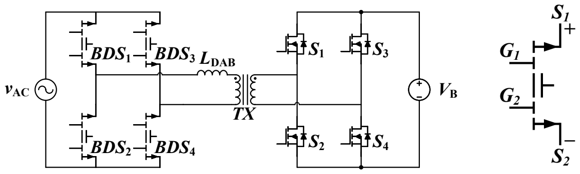

(a) (b)

Fig. 1. Schematic of (a) matrix type DAB single-stage OBC, (b) GaN MBDS.

Double-pulse testing (DPT) is the de facto method for quantifying device dynamic performance, including switching energies, dv/dt and di/dt limits, reverse-conduction behavior, and dynamic on-resistance [7]. While abundant DPT data exists for conventional GaN devices, evaluating MBDS under high-current conditions remains a critical gap, particularly for OBC applications. Because mainstream OBCs predominantly operate at $\geq$ 3 kW, full load switching currents routinely reach tens of amperes [8]. This lack of empirical data hinders the confident adoption of MBDS in single-stage OBCs, leaving unresolved questions regarding commutation asymmetry, safe operating margins, and practical gate-drive constraints.

This paper addresses this gap by:

- **Refining DPT for GaN MBDS:** A customized testing approach is introduced to overcome the limitations of traditional DPT methods for GaN MBDS.
- **Designing an optimized hardware testbed:** A dedicated DPT platform with minimized parasitic loop inductance is implemented. This layout mitigates severe voltage overshoots during high-current hard switching, preventing device breakdown and ensuring reliable testing.
- **Conducting a comprehensive comparative analysis:** The switching performance of GaN MBDS is systematically evaluated against conventional unidirectional GaN and SiC devices, providing practical guidance for single-stage OBC applications.

II. DPT Setup

A. Working Condition Analysis

Fig. 1(a) shows the schematic of a matrix-type DAB single-stage OBC, where $MBDS_1$–$MBDS_4$ and S_1–S_4 denote the primary- and secondary-side switches, respectively. The input AC voltage is v_{AC}, the output battery voltage is V_B. L_{DAB} is

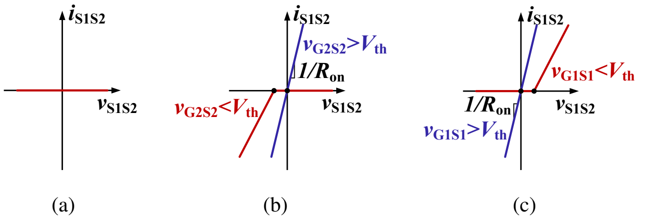

Fig. 2. Four quadrant MBDS behavior when (a) G_1, G_2 is low, (b) G_1 is high and (c) G_2 is high.

the DAB inductor, and TX is the transformer. Each MBDS features two independent gates, G_1 and G_2, as illustrated in Fig. 1(b). $v_{S_1S_2}$ is defined as the potential at S_1 relative to S_2.

When both G_1 and G_2 are held low, the MBDS blocks voltage bidirectionally-i.e., it remains off regardless of the polarity of $v_{S_1S_2}$. When G_1 is held high and G_2 is held low, the device provides forward-voltage blocking: it stays off for positive $v_{S_1S_2}$, but conducts in the third quadrant when $v_{S_1S_2}$ is negative and its magnitude exceeds the reverse threshold voltage V_{rev}, similar to a standard GaN HEMT. Conversely, when G_1 is held low and G_2 is held high, the MBDS provides reverse-voltage blocking: it remains off for negative $v_{S_1S_2}$, but conducts in the first quadrant when $v_{S_1S_2} > V_{\text{rev}}$, behaving like a GaN HEMT connected in reverse, as shown in Fig. 2.

Similar to a GaN HEMT, V_{rev} is related to the gate threshold voltage and the negative gate bias voltage in the off state

$$V_{\text{rev}} \approx V_{\text{th}} - V_{\text{gs,off}} + I \cdot R_{\text{rev}} \quad (1)$$

where V_{th} is the gate threshold voltage, $V_{\text{gs,off}}$ is the negative gate bias voltage in the off state, I is the current flowing through the MBDS during off state, R_{rev} is the equivalent conduction resistance. From (1), it can be inferred that, similar to a GaN HEMT, when conducting in reverse the MBDS's voltage drop V_{rev} is much larger than the body-diode drop of Si and SiC MOSFETs (typically about 0.7 V and 1.2 V, respectively). Consequently, the resulting losses are substantial, so this operating condition should be avoided as much as possible.

In the single-stage OBC shown in Fig. 1(a), the two primary-side MBDS half-bridges are both connected directly across the AC source. When the AC input voltage is in its positive half-cycle, i.e.

$$v_{\text{AC}}(t) > 0 \quad (2)$$

G_1, G_3, G_5, and G_7 are held high to avoid the reverse losses mentioned above, while G_2, G_4, G_6, and G_8 commutate at high frequency to form the primary-side square wave of the DAB. On the other hand, during the negative half-cycle, their roles swap: G_2, G_4, G_6, and G_8 stay held high, and G_1, G_3, G_5, and G_7 serve as the high-frequency primary full bridge signals.

When the input voltage reaches its peak, the voltage across the devices at turn-on/turn-off is at its maximum, i.e.

$$v_{\text{sw,max}} = v_{\text{AC,max}} = \sqrt{2} v_{\text{AC,nom.}} \quad (3)$$

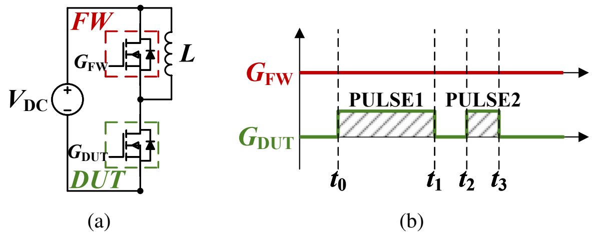

Fig. 3. (a) Circuit diagram and (b) gate drive signal of a conventional DPT for unidirectional devices.

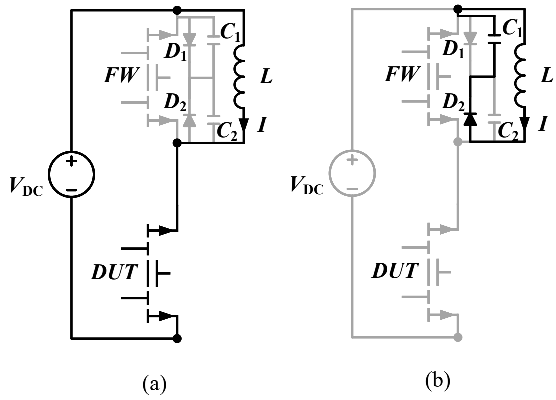

Fig. 4. Operation Mode Analysis of Conventional DPT on MBDS. (a) Pulse 1. (b) Freewheeling period.

where $v_{\text{AC,nom.}}$ is the nominal RMS voltage of the mains power supply. Owing to the PFC behavior of the single-stage OBC, the AC-side current also peaks at that instant.

B. MBDS DPT Customization

As shown in Fig. 3, in a conventional DPT configuration for unidirectional devices, the circuit primarily consists of the Device Under Test (DUT), a freewheeling device, a load inductor, and an external DC power supply. The freewheeling device can be a standard diode or an active switch i.e. a MOSFET. When an active switch is utilized, it remains in the off-state and conducts in the third quadrant, exhibiting reverse conduction characteristics similar to a diode. The freewheeling device is connected in parallel with the load inductor, and this combination is placed in series with the DUT. The external DC power supply (V_{DC}) is applied across the entire branch. During the DPT process, the gate drive signals are exclusively applied to the DUT. The freewheeling device does not require an active gate signal, as it relies entirely on its third-quadrant conduction capability. The testing sequence involves three specific stages:

1) **First Pulse:** The DUT is turned on, and the DC voltage (V_{DC}) is applied across the inductor, causing the inductor current to ramp up linearly to the desired test current level.
2) **Freewheeling Period:** The DUT is then turned off. During this interval, the continuous inductor current freewheels through the third quadrant of the freewheeling device.

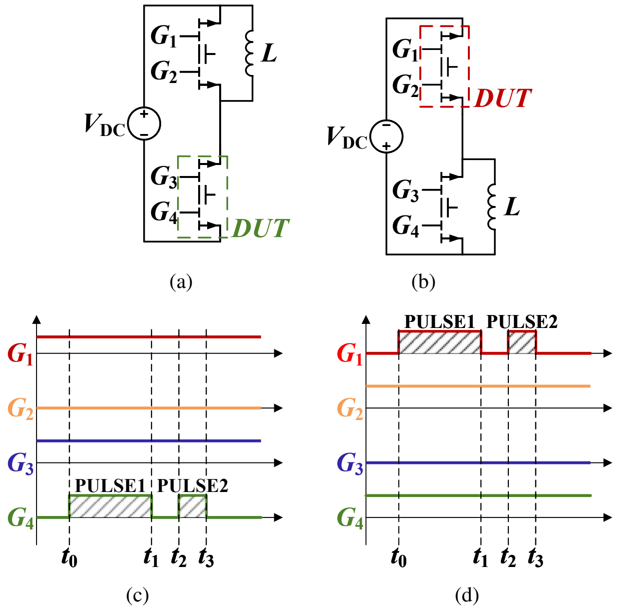

Fig. 5. (a) Positive-voltage and (b) negative-voltage DPTs circuit diagrams and (c) (d) their gate signal respectively.

3) **Second Pulse:** A second, shorter pulse is applied to the DUT. The transient voltage and current waveforms during the switching transitions of this pulse are captured to evaluate the turn-on and turn-off dynamic characteristics of the DUT at the established current level.

However, the conventional DPT methodology is fundamentally inadequate for characterizing the switching performance of GaN MBDS. When performing DPT with a GaN MBDS as the DUT, adopting the conventional driving logic will lead to critical system failures. In a standard DPT sequence, the DUT is completely turned off during the freewheeling period. However, based on the analysis in the previous subsection, the MBDS cannot passively conduct in the third quadrant when it is in the off-state. The third-quadrant conduction characteristics of the MBDS allow it to be modeled as an equivalent circuit comprising a pair of common-cathode diodes each in parallel with a body capacitance. Consequently, the inductor current abruptly loses its continuous freewheeling path. Under this condition, the entire inductor current is forced to charge C_1 , as shown in Fig. 4. This process causes an uncontrollable and rapid surge in the device's voltage, ultimately resulting in severe overvoltage and the catastrophic destruction of the device.

To address this critical limitation and avoid catastrophic device failure, adapts the DPT method with a customized gate drive sequence tailored for GaN MBDS devices. As shown in Fig. 5 (a), both the DUT and the freewheeling device utilize MBDS. Under a positive voltage supply, the low-side MBDS acts as the DUT while the high-side MBDS serves as the freewheeling device. Gates G_1 and G_3 are held high throughout the test to provide a continuous freewheeling path for the inductor current and to emulate realistic operating conditions. A standard 2-pulse signal, identical to that used in a conventional DPT, is applied to G_4 to control the turn-on and turn-off of the DUT, as illustrated in Fig. 5 (c).

Furthermore, as established in the previous subsection, the MBDS half-bridge in an OBC experiences alternating positive and negative voltage stresses during AC grid half-cycles. A comprehensive DPT methodology for MBDS must therefore include bipolar test conditions. Accordingly, a complementary negative-voltage test is performed, as shown in Fig. 5 (b): the high-side MBDS becomes the DUT, and the low-side MBDS acts as the freewheeling device. Gates G_2 and G_4 are held high throughout the test, and the 2-pulse signal is applied to G_1, as shown in Fig. 5 (d).

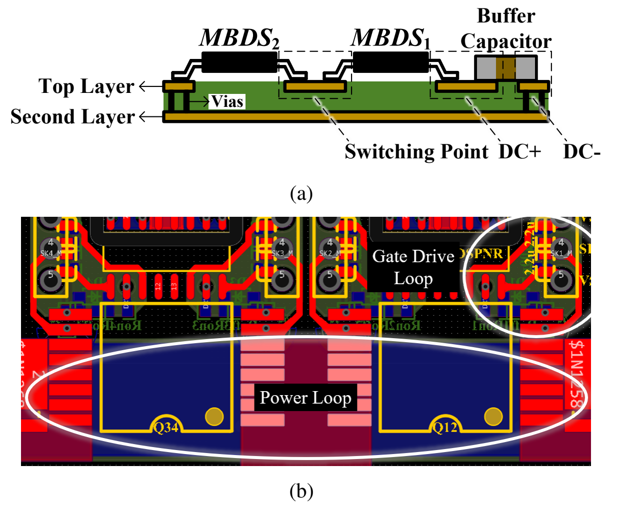

Fig. 6. (a) Lateral view, (b) top view of the optimized PCB layout using mutual inductance cancellation method.

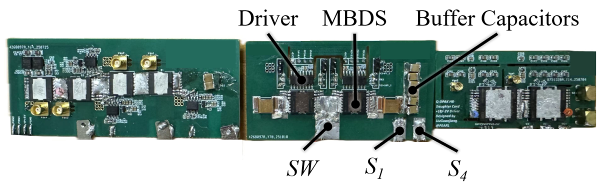

Fig. 7. DPT setup for the non-monolithic bidirectional switches half-bridge, the MBDS half-bridge and the SiC half-bridge.

C. Optimized Hardware Testbed Design

The MBDS device used for testing is the NV6428 from Navitas. For the gate driver of each MBDS, the NSI6602A-DSPNR isolated half-bridge driver from NOVOSENSE is selected, each of which can output two isolated gate drive signals to drive one MBDS, sourcing 4 A and sinking 6 A peak current. To address the issue of false turn-on caused by the low turn-on gate voltage threshold V_{th} of GaN HEMTs, the drive power supply adopts a negative off-state voltage bias, where the gate voltage is -3.8 V during the off state. Three different gate resistor values (i.e. 20 Ω, 33 Ω, and 47 Ω) are selected to test the differences in MBDS dynamic performance under different gate resistances.

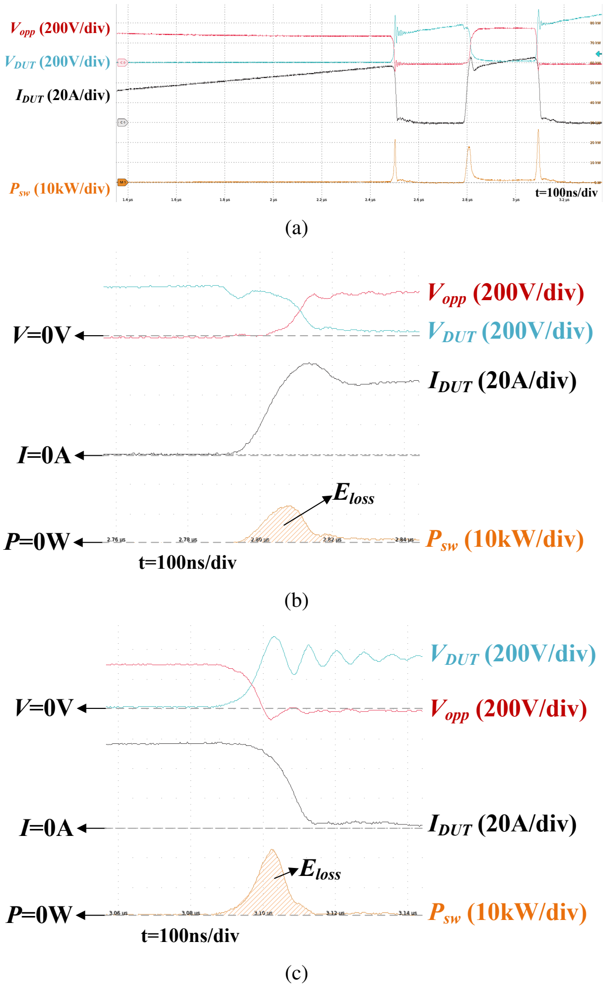

Fig. 8. (a) The key waveforms of the positive-voltage DPT under $375V\&50A$ condition and detailed waveforms of (b) turn-on, (c) turn-off transients.

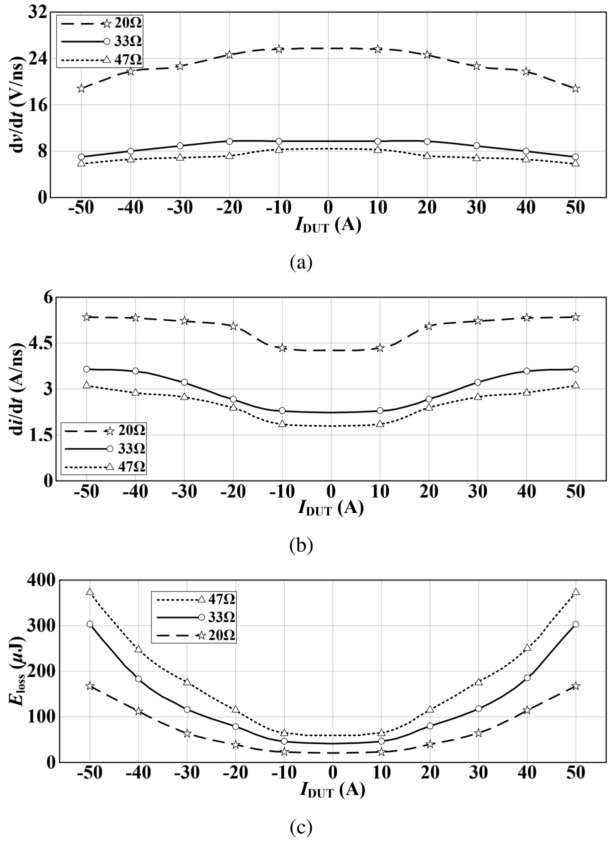

Fig. 9. (a) dv/dt, (b) di/dt and (c) switching energy of the turn-on transient under different operating currents and gate resistance.

Fig. 6 shows the layout of the MBDS half-bridge power loop and gate drive loop, minimizing parasitic inductance in the power loop to reduce hard-switching voltage overshoot [9]. The direction of the power loop on the top layer is from right to left, and it enters the second layer through vias located on the left side of $MBDS_2$. On the second layer, the direction of the power loop is from left to right. The power loop directions on the top and second layers are opposite, and the parasitic inductances in the loops generate mutual inductance that cancels each other out, resulting in a lower total loop parasitic inductance. Vertically, there is no area overlap and mutual coupling between the gate drive loop and the power loop, which prevents the generation of parasitic capacitance. An air core inductor with an inductance value of 14 μH was selected for the DPT experiment, so as to avoid saturation. According to (2), for an input of 85-265 VAC, the maximum peak voltage is approximately 375 V; therefore, the DPT power supply voltage V_{DC} is set to 375 V. Taking into account the 6.6 kW OBC power rating and the rated current of NV6428, the switching current for the DPT is set to 50 A max.

For comparison, additional DPTs are conducted on a SiC half-bridge and on a four-quadrant switch half-bridge formed by connecting four GaN HEMTs in two common-drain anti-series pairs (hereinafter referred to as non-monolithic GaN bidirectional switches), both of which adopt UCC5350, a single channel isolated driver that can source 5 A and sink 5 A, as the gate driver. A gate resistor value of 33 Ω is selected. As shown in Fig. 7, from left to right are images of the DPT test platforms for the non-monolithic GaN bidirectional switch half-bridge, the MBDS half-bridge, and the SiC half-bridge. All three DPT platforms adopt the same mutual inductance cancellation method mentioned above, and loop parasitic inductance is minimized. A Rogowski coil is used for current measurement, while high-voltage differential probes with high Common Mode Rejection Ratio (CMRR) are used for voltage measurement.

III. Experimental Results

The key waveforms at 50 A switching current in positive-voltage DPT are shown in Fig. 8. V_{DUT} denotes the voltage across the DUT, V_{opp} the voltage across the other MBDS used for freewheeling inductor current, I_{DUT} the current flowing through the DUT, and P_{DUT} the product of V_{DUT} and I_{DUT}, which is used to calculate the DUT's switching losses

$$E_{\mathrm{loss}} = \int V_{\mathrm{DUT}} \cdot I_{\mathrm{DUT}} = \int P_{\mathrm{DUT}} \tag{4}$$

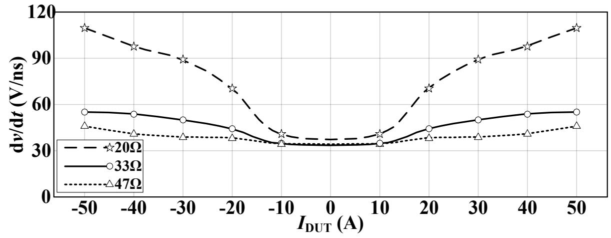

(a)

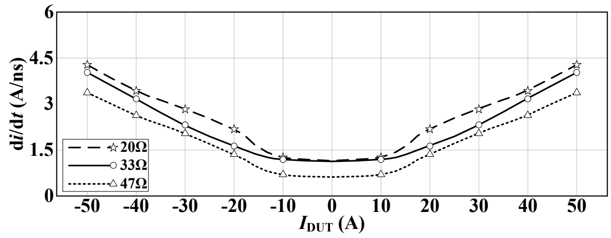

(b)

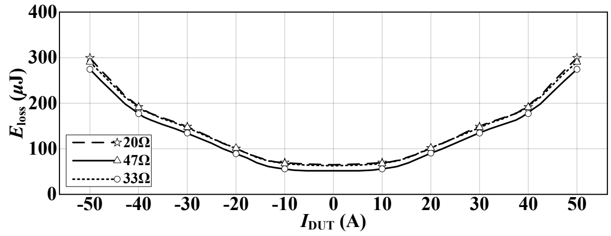

(c)

Fig. 10. (a) dv/dt, (b) di/dt and (c) switching energy of the turn-off transient under different operating currents and gate resistance.

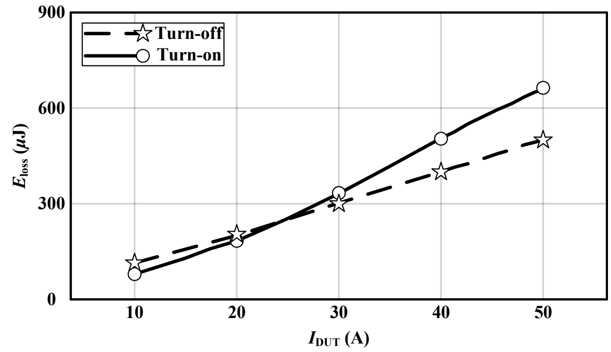

Fig. 11. Switching energy loss of SiC.

The positive-voltage and negative-voltage DPTs are conducted under different switching current and gate resistance, and the switching dv/dt, di/dt and energy loss in both tests are as shown in Fig. 9 and Fig. 10. From the experimental results, the following conclusions can be drawn:

- The MBDS exhibited good symmetry i.e. at the same switching current, the switching dv/dt, di/dt and energy loss in both positive-voltage and negative-voltage DPTs were nearly identical.
- During turn-on, the increasing of switching current has little effect on turn-on speed. As the switching current increases, the MBDS turn-on dv/dt decreases slightly and di/dt increases slightly, but both changes are small; therefore, turn-on loss increases significantly with higher switching current. In addition, reducing the turn-on gate resistance markedly increases the MBDS turn-on speed, leading to a significant reduction in turn-on loss. Thus, a smaller turn-on gate resistance is recommended for MBDS.
- During turn-off, larger switching current leads to higher turn-off dv/dt, di/dt, and switching loss. Comparing the dv/dt during turn-on and turn-off shows that MBDS turns off much faster than it turns on. Reducing the turn-off gate resistance has little impact on turn-off di/dt and turn-off loss, but it results in a higher dv/dt. However, an excessively large turn-off gate resistance can cause unintended turn-off of the device, leading to device failure. Therefore, a moderate turn-off gate resistance is recommended for MBDS.

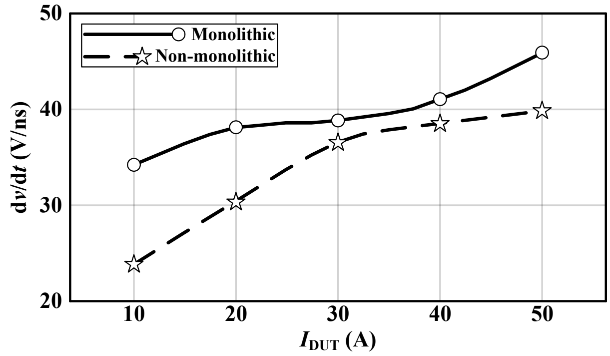

(a)

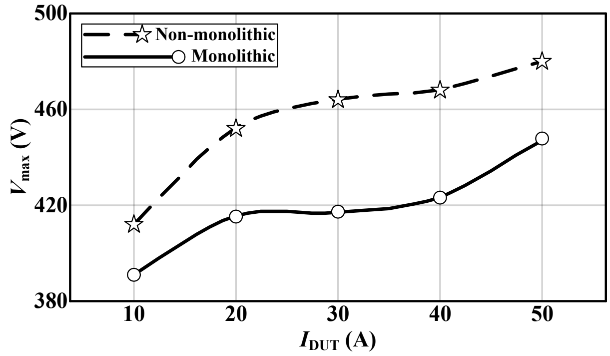

(b)

Fig. 12. (a) dv/dt and (b) v_{DUT} overshoot of monolithic and non-monolithic BDS.

Performing a DPT on the SiC half-bridge shown in Fig. 5 yields the switching losses at different switching currents, as shown in Fig. 11. Comparing the results of MBDS and SiC indicates that MBDS, as a GaN device, inherently exhibits faster switching speed and therefore lower switching losses.

Before the advent of MBDS, the non-monolithic bidirectional switch shown in Fig. 7 was a mainstream implementation of a four-quadrant switch. Compared with it, MBDS inherently saves half the PCB area and, because its power loop is only half as long, features lower loop parasitic inductance, resulting a lower hard switch voltage overshoot. A DPT on the non-monolithic bidirectional switch shows that its turn-off speed is not as fast as that of an MBDS with a 47 Ω gate resistor, whereas its voltage overshoot is far greater than that of MBDS, as shown in Fig. 12. This verifies MBDS's advantage in parasitic parameters.

IV. Conclusion

This paper proposes a customized DPT with tailored gate sequence to safely evaluate GaN MBDSs up to 50 A and 375 V, preventing the destructive overvoltage inherent in conventional DPT setups. Using an optimized testbed with mutual inductance cancellation, the results demonstrate that GaN MBDSs exhibit highly symmetrical switching under bipolar voltage stress. The MBDS exhibits lower switching losses compared to SiC devices and significantly reduced voltage overshoot compared to non-monolithic GaN equivalents. Finally, the characterization reveals that utilizing a small turn-on gate resistance and a moderate turn-off gate resistance optimizes dynamic performance, providing practical guidance for adopting MBDSs in high-density single-stage on-board chargers.

References

[1] H. Wouters and W. Martinez, "Bidirectional Onboard Chargers for Electric Vehicles: State-of-the-Art and Future Trends," in IEEE Transactions on Power Electronics, vol. 39, no. 1, pp. 693-716, Jan. 2024.

[2] J. Everts, F. Krismer, J. Van den Keybus, J. Driesen and J. W. Kolar, "Optimal ZVS Modulation of Single-Phase Single-Stage Bidirectional DAB AC–DC Converters," in IEEE Transactions on Power Electronics, vol. 29, no. 8, pp. 3954-3970, Aug. 2014.

[3] P. Nayak, K. Rajashekara and S. K. Pramanick, "Soft-Switched Modulation Technique for a Single-Stage Matrix-Type Isolated DC–AC Converter," in IEEE Transactions on Industry Applications, vol. 55, no. 6, pp. 7642-7656, Nov.-Dec. 2019.

[4] R. Kumar and B. Singh, "Matrix Converter Based Single Stage Bidirectional On-Board EV Charger with Reactive Power Support," 2020 IEEE International Conference on Power Electronics, Smart Grid and Renewable Energy (PESGRE2020), Cochin, India, 2020.

[5] U. Raheja et al., "Applications and characterization of four quadrant GaN switch," 2017 IEEE Energy Conversion Congress and Exposition (ECCE), Cincinnati, OH, USA, 2017, pp. 1967-1975.

[6] J. Huber and J. W. Kolar, "Monolithic Bidirectional Power Transistors," in IEEE Power Electronics Magazine, vol. 10, no. 1, pp. 28-38, March 2023.

[7] D. Goldmann, S. Mayer, S. Schramm and H. -G. Herzog, "Comparing Switching and Conduction Losses of Uni- and Bidirectional SiC Semiconductor Switches for AC Applications," 2021 23rd European Conference on Power Electronics and Applications (EPE'21 ECCE Europe), Ghent, Belgium, 2021, pp. P.1-P.9.

[8] Q. Song, H. Cui, Q. Li and Y. Zhang, "Impact of Substrate Bias on the Stability of Bidirectional GaN HEMT in Hard-and Soft-Switching," 2025 IEEE Applied Power Electronics Conference and Exposition (APEC), Atlanta, GA, USA, 2025, pp. 202-206.

[9] E. Persson, "Optimizing PCB Layout for HV GaN Power Transistors," in IEEE Power Electronics Magazine, vol. 10, no. 2, pp. 65-78, June 2023.